Ellipsoidal Relaxation of Deformed Vesicles

Miao Yu, Rafael B. Lira, Karin A. Riske, Rumiana Dimova, and Hao Lin

Phys. Rev. Lett. **115**, 128303 — Published 18 September 2015

DOI: 10.1103/PhysRevLett.115.128303

Ellipsoidal Relaxation of Deformed Vesicles

Miao Yu,[1] Rafael B. Lira,[2,3] Karin A. Riske,[3] Rumiana Dimova,[2,*] and Hao Lin[1,†]

[1]*Department of Mechanical and Aerospace Engineering, Rutgers, The State University of New Jersey, 98 Brett Road, Piscataway, NJ 08854, USA*

[2]*Department of Theory and Bio-Systems, Max Planck Institute of Colloids and Interfaces, Science Park Golm, 14424 Potsdam, Germany*

[3]*Department of Biophysics, Federal University of São Paulo, BR-04044020 Sao Paulo, Brazil*

(Dated: August 11, 2015)

Theoretical analysis and experimental quantification on the ellipsoidal relaxation of vesicles are presented. The current work reveals the simplicity and universal aspects of this process. The Helfrich formula is shown to apply to the dynamic relaxation of moderate-to-high tension membranes, and a closed-form solution is derived which predicts the vesicle aspect ratio as a function of time. Scattered data are unified by a timescale, which leads to a similarity behavior, governed by a distinctive solution for each vesicle type. Two separate regimes in the relaxation are identified, namely, the "entropic" and the "constant-tension" regime. The bending rigidity and the initial membrane tension can be simultaneously extracted from the data/model analysis, posing the current approach as an effective means for the mechanical analysis of biomembranes.

PACS numbers: 82.70.Uv, 47.63.mf, 87.16.D-, 87.85.G-

The mechanics of lipid membrane is essential to many fundamental biological processes such as signal transduction, vesicle trafficking, membrane fusion, mechanosensing, and ion channel gating [1]. Giant unilamellar vesicles (GUVs) with dimensions of living cells and controlled membrane composition constitute ideal model systems to characterize the properties of lipid assemblies [2]. A variety of techniques have been developed to probe vesicle mechanics, including AFM [3], optical and magnetic stretching [4, 5], micropipette aspiration [6], tether pulling [7], shear-flow-based deformation [8], fluctuation spectroscopy [9], and electrodeformation [10–12]. In each case (except fluctuation spectroscopy), the common strategy is to investigate the deforming response of the membrane via the application of external forcing. Mechanical properties such as the bending rigidity and elastic modulus can be extracted via model analysis, e.g., of the force-deformation relation [13–16]. These studies shed significant insight on the lipid membrane as a soft material, and provide powerful analytical tools for its mechanical characterization. Meanwhile, challenges remain, such as complex contact geometries between the probe and the membrane which lead to singularity and complexity in model analysis, low through-put, and the requirement of sophisticated instrumentations.

The current work does not attempt to present another deformation-based technique. Instead, we bring to the focus light an aspect previously overlooked, namely, the relaxation after removal of external forcing. In this process, the dynamics is left to the mere devices of membrane retraction and responsive fluid motion, and the physical problem is thus significantly simplified. Relaxation has been broadly analyzed in other fields such as polymer science [17–19] and droplet dynamics [20, 21]. However, for vesicles (and in general for biological cells), it has been a long-ignored aspect, and investigations are scarce in comparison with the extensive amount of work on the deformation. Prior studies were either phenomenological and in the absence of a quantitative modeling [22–24], or accessorial to deformation analysis and for a limited few cases [16, 25, 26]. The fundamental merit of relaxation analysis and its significance have been thus far elusive, due to the lack of attention and systematic measurements. In contrast, the current work posts the first relaxation study combining a quantitative theory with controlled experiments, with which we unveil the particularly simplistic behavior and universal aspects of this process. The contributions are as follows. First, we derive a closed-form solution for the dominantly observable mode, namely, the ellipsoidal mode. Second, we produce extensive data for different vesicle types, which provides the basis for our analysis. Third, the scattered data is unified by considering an important timescale, which leads to a similarity behavior, governed by a unique solution. This solution serves as the hallmark for each vesicle type (or each value of bending rigidity). Fourth, two distinctive regimes are identified, namely, the "entropic" regime, and the "constant-tension" regime, controlled by different physical parameters. Last but not least, both the intrinsic property, the bending rigidity, and the extrinsic property, the initial membrane tension, can be simultaneously extracted and differentiated. The current approach thus may be developed into an effective method for the mechanical analysis of lipid or polymer membranes, for vesicles, and eventually for cells and other biomembranes.

We begin with the basic assumptions the analysis pred-

*Corresponding author: Rumiana.Dimova@mpikg.mpg.de
†Corresponding author: hlin@jove.rutgers.edu

icates on: a) Assuming that the vesicle is deformed from an initially spherical state, the vesicle then remains ellipsoidal in its apparent shape during relaxation, and relaxes back to a sphere. This assumption follows many direct observations [11, 22], and is justified via Fourier analysis of the image contours (see Supplemental Material (SM) for details). b) The vesicle volume is conserved. Under these two assumptions, the membrane contour is described by a single Legendre polynomial, $r = r_0[1+(2/3)\epsilon P_2(\cos(\theta))]$. Here (r, θ, ϕ) defines a spherical coordinate system, r_0 is the vesicle radius in the spherical state, and $P_2(x) = (3x^2 - 1)/2$. The shape factor, ϵ, is related to the vesicle aspect ratio by $\epsilon = a/b - 1$, where a and b are the lengths of the major and minor axes, respectively. The evolution equation for the relaxation of ϵ can be derived following the analysis of Seifert for quasi-spherical shapes [26, 27], by removing the deforming external flow field in the governing equation of the P_2 mode (SM):

$$\frac{\mathrm{d}\epsilon}{\mathrm{d}\tau} = -C\epsilon \exp\left(\frac{8\pi\kappa\Delta}{k_B T}\right), \quad \tau = \frac{t}{t_D},\ t_D = \frac{r_0\mu_e}{\Gamma_0}, \quad (1)$$

$$C = 24/(32 + 23\mu_r), \quad \mu_r = \mu_i/\mu_e. \quad (2)$$

Here t is time. Γ_0 is the membrane tension in the spherical state, which we term "initial membrane tension". μ_i and μ_e are the intra- and extra-vesicular viscosity, respectively. κ is the bending rigidity, k_B is the Boltzmann constant, and T is temperature. Δ is the increase in the apparent membrane area relative to the spherical state. In adopting Eq. (1), we have assumed that P_2 is the dominant mode giving rise to the apparent vesicle shape, whereas all other modes of the spherical harmonics have relaxed to thermal fluctuations according to the Langevin equation [27]. Finally, the celebrated Helfrich model effectively manifests itself in Eq. (1) via

$$\Gamma/\Gamma_0 = \exp(8\pi\kappa\Delta/k_B T), \quad (3)$$

where Γ is the membrane tension corresponding to a deformed state [28]. In this model, membrane tension increases/decreases in response to the unfolding/folding of the "undulations" (thermal fluctuations) on the membrane. Importantly, Eq. (3) is directly derived from the total membrane area constraint in [27]. Previously, the Helfrich formula only applies to equilibrium shapes. However, we demonstrate that for moderate-to-high membrane tension ($\gtrsim 10^{-7}$ N/m), and due to the fast relaxation timescale of the higher modes and the low percentage of area stored in the lower fluctuation modes, this equilibrium formula can be extended to study dynamic situations such as in relaxation (SM). The current work henceforth complements fluctuation microscopy which is appropriate for low-tension ($\sim 10^{-9} - 10^{-8}$ N/m) membranes [9, 12, 29].

A salient feature of Eq. (1) is that in a dimensionless form, it is an autonomous ODE for ϵ, because Δ is exclusively a function of ϵ. This feature implies that once properties such as κ, μ_i and μ_e are known, the solution to this equation is unique. Furthermore, this solution can be attained in a closed form if one recognizes that via Taylor expansion, $\Delta = 8\epsilon^2/45 + O(\epsilon^3)$. Substituting this expression into (1) and ignoring the $O(\epsilon^3)$ term, we arrive at an analytical solution after integration,

$$E_1(\alpha\epsilon^2) = E_1(\alpha\epsilon_0^2) + 2C\tau, \quad (4)$$

where $\alpha \equiv 64\pi\kappa/45k_B T$, and ϵ_0 is the value for ϵ at $\tau = 0$, the beginning point of relaxation. Here E_1 is the exponential integral function encountered regularly in biophysical or physical problems [30, 31]. When the vesicle approaches sphericity, namely, $\epsilon \to 0$, $E_1(\alpha\epsilon^2) \sim -\ln(\alpha\epsilon^2)$. Eq. (4) becomes simply

$$\epsilon = \epsilon_0 \exp(-C\tau). \quad (5)$$

Equation (5) is similar to the relaxation equation for droplets [20], with a slightly differing factor, C (see SM). Based on Eqs. (4, 5), two regimes of relaxation can be readily delineated. The first is the "entropic" regime: for higher values of ϵ, the trend of the solution is controlled by the bending rigidity since the membrane tension depends strongly (exponentially) on the apparent surface area. Relaxation eventually reduces ϵ to be sufficiently small, so that the "constant-tension" regime is reached. In this regime, because $\Delta \sim O(\epsilon^2)$, the Helfrich constitutive relation (3) is weak, and $\Gamma \approx \Gamma_0$ to the leading order. In this case, Eq. (5) is equivalently obtained by integrating Eq. (1) while setting $\Delta = 0$. Equation (4) provides a simple and convenient approximate solution to the original ODE (1), and is employed in the ensuing data analysis. A validation of its accuracy is included in the SM.

To test the theory, 1-palmitoyl-2-oleoyl-sn-glycero-3-phosphocholine (POPC) vesicles, pure or mixed with cholesterol of 10, 20 and 30% in mole fraction, were formed using standard electroformation technique, and were deformed with DC electric pulses following protocols developed in our previous work (SM) [22, 32]. This particular technique is chosen due to its advantage of the lack of direct contact with the vesicle. However, the general methodology presented in this work could be applied to relaxation induced by any other type of deformation trigger insofar as the vesicle remains approximately ellipsoidal. Representative images of the deformation-relaxation process are shown in Fig. 1. In Fig. 1a, the vesicle was in its initial, spherical state. An applied pulse (1.6 kV/cm, 100 μs) elongated the vesicle (b) until it reached maximum deformation (c). The vesicle then relaxed after the pulse ceased (d, e), and eventually restored sphericity (f). Each vesicle image is fitted with an elliptical shape (see c), from which a and b are extracted.

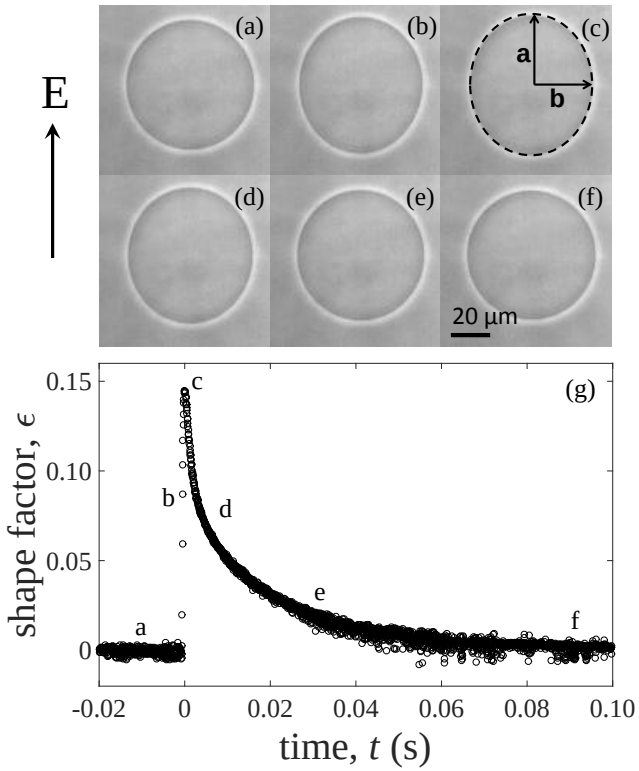

FIG. 1: (a)-(f) Representative phase-contrast images of a POPC vesicle deformed with a DC electric pulse. (g) ϵ is defined as $a/b-1$, and is shown as a function of time.

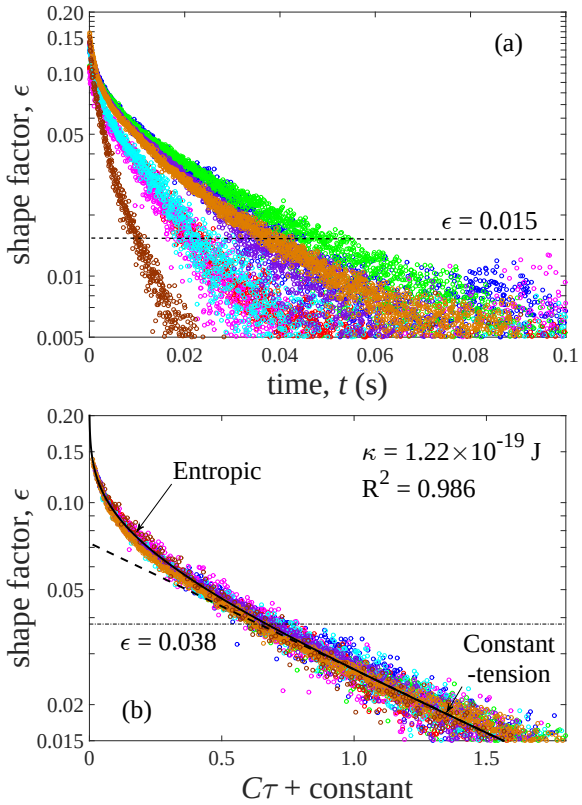

FIG. 2: Relaxation of POPC vesicles. (a) ϵ is shown for 8 different vesicles denoted by different colors. (b) Time normalization and translation leads to collapse of all data in (a). The solid curve is theoretical prediction with Eq. (4). The dashed curve is a guide for the eye, $\epsilon \sim \exp(-C\tau)$. A "constant" in the time label denotes translation.

Other shape modes are negligible as we demonstrate in the SM. In g, ϵ is shown as a function of time, where the approximate locations of a-f are noted. Successful model predictions on electrodeformation have been developed elsewhere [16, 26, 33], whereas here we focus on relaxation.

Figure 2a shows the relaxation of 8 POPC vesicles resulting from deformation induced via different pulsing parameters. The short pulse duration and low voltage ensured the absence of membrane poration (see Table S2 in the SM). Importantly, we carefully evaluated and ruled-out the effects of membrane-discharging during relaxation (SM). The data is seemingly scattered, but the behavior is qualitatively similar. On a logarithmic scale, ϵ experiences a relatively rapid initial decrease, followed by an asymptotic approach to linearity with respect to time. The similarity invites attempts to collapse the data via non-dimensionalization. In fact, we already demonstrated above that once κ, μ_i, and μ_e are given, relaxation follows a unique solution as a function of the dimensionless time, τ. This solution unites the data regardless of the original state of the vesicle, namely, initial tension, Γ_0, and radius, r_0; and the starting point of relaxation, ϵ_0, since the governing ODE is autonomous. The result is demonstrated in Fig. 2b. For each set of data, the dimensional (physical) time, t, is first normalized with t_D to obtain τ (Eq. (1)). The data sets are also allowed to translate horizontally for alignment, a standard operation for an autonomous system without altering the governing physics (SM). We observe that the 8 data sets are now in concurrence with each other in dimensionless form, and are well captured by a theoretical solution produced with Eq. (4). In generating results in Fig. 2b, the values of both Γ_0 (to calculate t_D) and κ are needed, and are obtained by minimizing the error between the data sets and the theoretical solution. The bending rigidity, κ, is assumed to be the same for all 8 vesicles, and is found to be 1.22×10^{-19} J. Values of Γ_0 differ for each vesicle; these and all pertinent parameters are found in Table S2 of the SM. An excellent agreement is indicated by the value of the coefficient of determination, $R^2 = 0.986$. The data analysis and results are extensively validated, especially by comparing three different methodologies. Note that large fluctuations are observed for $\epsilon \lesssim 0.015$, due to thermal noise and limitations in the imaging system. This part of the data is consistently discarded in Fig. 2b and all results to follow. Details of the methods and a discussion on the cut-off threshold is found in the SM.

Some further remarks on Fig. 2b are appropriate.

First, the presence of the regimes as suggested by the theory is evident. We observe that for $\epsilon \lesssim 0.038$, all vesicles relax exponentially according to Eq. (5). On the other hand, for $\epsilon \gtrsim 0.038$, the deviation from the exponential behavior is dictated by the Helfrich constitutive relation. The separation of the regimes is schematically delineated by a dot-dashed line. The determination of the threshold value is discussed later. Second, in the analysis above we have effectively presented a method to simultaneously extract κ and Γ_0. The former is an intrinsic membrane property, and the value from our analysis, 1.22×10^{-19} J, agrees well with that from the literature ($0.39 - 1.6 \times 10^{-19}$ J [13]). The initial membrane tension, Γ_0, is a non-intrinsic property that depends on the history of every vesicle and can be modulated by means such as changes in the extra- and intra-vesicular osmolarity. Our approach is simple and convenient when compared with many alternatives, in particular when considering the closed-form solutions (4, 5).

The same analysis on additional data is presented in Fig. 3. Altogether 5 groups are shown. The POPC data is identical to those shown in Fig. 2b, presented here for reference. Data for POPC with 10%, 20%, and 30% of cholesterol contain 8, 7, and 6 vesicles, respectively. Data for each vesicle type is normalized following the approach above, and then translated so that they are aligned in the last stage, i.e., in the constant-tension regime. Solid lines represent the theoretical prediction for each case. We observe again the similarity pattern for each vesicle type. In addition, as the cholesterol concentration increases, the initial descent of the relaxation in the entropic regime becomes successively steeper, indicating an increase in the value of κ. Indeed, they are found to be 1.73, 1.90, and 2.18×10^{-19} J, respectively. These numbers corroborate the trend in the measurements by Henriksen et al. [29] using fluctuation spectroscopy, namely, 2.24, 2.89 and 3.57×10^{-19} J for POPC vesicles with 10%, 20%, and 30% cholesterol (mole fraction), respectively. The differences in the values of κ are attributed to those in the specific experimental conditions, especially the sugar concentrations [13]. However, as the constant-tension regime is reached with lower values of ϵ, all vesicles converge to the linear (exponential) behavior.

Particular to electrodeformation, we also present another group of data, namely, electroporated POPC vesicles (filled triangles). Poration was induced by stronger and longer pulses (Table S6). In this case, all 4 sets of relaxation data follow a pure exponential decay. This result is interesting but not surprising, as for an electroporated membrane, area expansion/contraction can be mediated by that of electropores, and the Helfrich constitutive relation is therefore lost. Detailed parameters for all vesicles in Fig. 3 are listed in Tables S2-S6 in the SM.

Importantly, the transition value of ϵ between the entropic and constant-tension regimes does depend on κ,

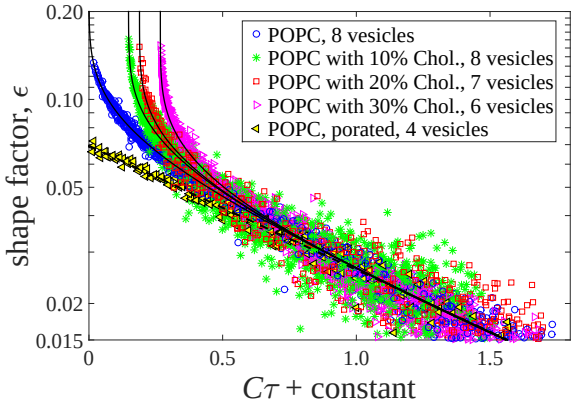

FIG. 3: Relaxation of POPC vesicles with various cholesterol mole fractions, and electroporated POPC vesicles. The solid and dashed lines are theoretical predictions. The values of R^2 are 0.986 (pure POPC), 0.942 (10%), 0.964 (20%), 0.985 (30%), and 0.993 (porated).

as depicted in Fig. 4 in the phase space of κ and ϵ. The two regimes are separated by the solid line using $\exp(8\pi\kappa\Delta/k_BT) = 1.2$. Note that the choice of 1.2 is empirical: it is a number indicating an appreciable deviation from the constant-tension regime. Considering that $\Delta \cong 8\epsilon^2/45$, we have $\kappa\epsilon^2 \cong 1.75 \times 10^{-22}$ J as an approximate guideline. To the far right, we also present the elastic regime, which occurs for large deformations where all fluctuations are flattened. In this case, the intermolecular spacing of the lipids does change, and elastic stretching becomes appreciable. For this regime, an extension of the Helfrich model needs to be used instead of (3), $\Delta = \frac{k_BT}{8\pi\kappa} \ln\left(\frac{\Gamma}{\Gamma_0}\right) + \left(\frac{\Gamma}{\Gamma_0} - 1\right) \frac{\Gamma_0}{K_a}$ [28]. Here K_a is the bulk elastic modulus of the membrane, and the first and second terms on the RHS denote contributions from entropic and elastic stretching, respectively. The dashed lines in Fig. 4 are calculated by setting equal the two competing contributions, for three representative values of K_a/Γ_0, namely, 10^4, 10^5 and 10^6, using $K_a \simeq 0.2$ N/m [34] and $\Gamma_0 \simeq 0.2 - 20 \times 10^{-6}$ N/m (SM). In Fig. 4, each symbol represents a pair of (ϵ_0, κ), for the vesicles presented in the first four groups in Fig. 3. Evidently, all vesicles in the current study do not reach the stretching regime.

In a brief summary, this work reveals the simplistic behavior of ellipsoidal relaxation of GUVs, and elucidates its characteristics. A closed-form solution lends further power to the analysis, and serves as a unique hallmark for each vesicle type. The methodology can be potentially extended to study important mechanical problems of biological cells. For example, both bending rigidity and membrane tension are found to play critical roles in nanoparticle-cell membrane interaction [35]. The current approach promises consistent and specific property differentiation, in contrast to the deformation-based, bulk-averaged measurements [36]. The model is currently lim-

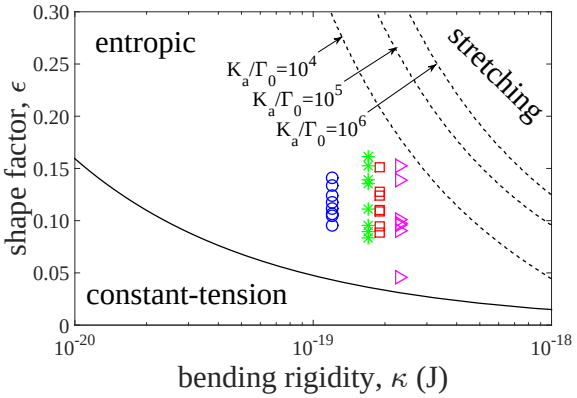

FIG. 4: Regimes of relaxation in the phase space of ϵ and κ. Each symbol represents a pair of (ϵ_0, κ) (or a vesicle) for data in Fig. 3, with the same legend.

ited to membranes with negligible viscosity as in fluid lipid membranes, and does not capture any rheological behavior therein. However, such extension can be incorporated [26]. Last but not least, the relaxation analysis may be applied to study vesicles/membranes deformed with means other than electric fields.

HL acknowledges funding support from NSF CBET-0747886 and NSFC 11328201. KAR and RBL acknowledge support from FAPESP. The authors gratefully acknowledge constructive discussions with P. Vlahovska.

[1] D. Boal, *Mechanics of the Cell, Second Edition* (Cambridge University Press, 2012).
[2] R. Dimova, *Giant vesicles: a biomimetic tool for membrane characterization*, edited by A. Iglic, Advances in Planar Lipid Bilayers and Liposomes, Vol. 16 (Elsevier Inc., 2012) pp. 1–50.
[3] Q. Chen, H. Schönherr, and G. J. Vancso, Soft Matter **5**, 4944 (2009).
[4] O. Sandre, C. Ménager, J. Prost, V. Cabuil, J.-C. Bacri, and A. Cebers, Phys. Rev. E **62**, 3865 (2000).
[5] M. E. Solmaz, R. Biswas, S. Sankhagowit, J. R. Thompson, C. A. Mejia, N. Malmstadt, and M. L. Povinelli, Biomed. Opt. Express **3**, 2419 (2012).
[6] E. Evans and W. Rawicz, Phys. Rev. Lett. **64**, 2094 (1990).
[7] V. Heinrich and R. E. Waugh, Ann. Biomed. Eng. **24**, 595 (1996).
[8] M. Abkarian and A. Viallat, Biophys. J. **89**, 1055 (2005).
[9] P. Méléard, T. Pott, H. Bouvrais, and J. Ipsen, Eur. Phys. J. E **34**, 116 (2011).
[10] M. Kummrow and W. Helfrich, Phys. Rev. A **44**, 8356 (1991).
[11] R. Dimova, K. A. Riske, S. Aranda, N. Bezlyepkina, R. L. Knorr, and R. Lipowsky, Soft Matter **3**, 817 (2007).
[12] R. S. Gracia, N. Bezlyepkina, R. L. Knorr, R. Lipowsky, and R. Dimova, Soft Matter **6**, 1472 (2010).
[13] R. Dimova, Adv. Colloid Interface Sci. **208**, 225 (2014).
[14] D. Marsh, Chem. Phys. Lipids **144**, 146 (2006).
[15] W. Rawicz, K. C. Olbrich, T. McIntosh, D. Needham, and E. Evans, Biophys. J. **79**, 328 (2000).
[16] J. Zhang, J. D. Zahn, W. Tan, and H. Lin, Phys. Fluids **25**, 071903 (2013).
[17] S. Gerashchenko and V. Steinberg, Phys. Rev. Lett. **96**, 038304 (2006).
[18] R. D. Priestley, C. J. Ellison, L. J. Broadbelt, and J. M. Torkelson, Science **309**, 456 (2005).
[19] S.-Q. Wang, S. Ravindranath, P. Boukany, M. Olechnowicz, R. P. Quirk, A. Halasa, and J. Mays, Phys. Rev. Lett. **97**, 187801 (2006).
[20] S. Guido and M. Villone, J. Colloid Interface Sci. **209**, 247 (1999).
[21] M. Tjahjadi, J. M. Ottino, and H. A. Stone, AlChE J. **40**, 385 (1994).
[22] K. A. Riske and R. Dimova, Biophys. J. **88**, 1143 (2005).
[23] P. K. Wong, W. Tan, and C. M. Ho, Biomech. J. **38**, 529 (2005).
[24] V. Kantsler, E. Segre, and V. Steinberg, Phys. Rev. Lett. **101**, 048101 (2008).
[25] H. Zhou, B. B. Gabilondo, W. Losert, and W. van de Water, Phys. Rev. E **83**, 011905 (2011).
[26] P. F. Salipante and P. M. Vlahovska, Soft Matter **10**, 3386 (2014).
[27] U. Seifert, Eur. Phys. J. B **8**, 405 (1999).
[28] W. Helfrich and R. M. Servuss, Il Nuovo Cimento **3D**, 137 (1984).
[29] J. Henriksen, A. C. Rowat, and J. H. Ipsen, Eur. Biophys. J. **33**, 732 (2004).
[30] H. Gao, W. Shi, and L. B. Freund, Proc. Natl. Acad. Sci. U.S.A. **102**, 9469 (2005).
[31] P.-H. Tseng and T.-C. Lee, J. Hydrol. **205**, 38 (1998).
[32] K. A. Riske and R. Dimova, Biophys. J. **91**, 1778 (2006).
[33] P. M. Vlahovska, R. S. Gracia, S. Aranda-Espinoza, and R. Dimova, Biophys. J. **96**, 4789 (2009).
[34] J. R. Henriksen and J. H. Ipsen, Eur. Phys. J. E **14**, 149 (2004).
[35] X. Yi, X. Shi, and H. Gao, Nano Lett. **14**, 1049 (2014).
[36] S. Suresh, J. Spatz, J. P. Mills, A. Micoulet, M. Dao, C. T. Lim, M. Beil, and T. Seufferlein, Acta Biomaterialia **1**, 15 (2005).
[37] See Supplemental Material at [URL] for Refs. [38-42].
[38] G. Niggemann, M. Kummrow, and W. Helfrich, J. Phys. II France **5**, 413 (1995).
[39] J. T. Schwalbe, P. M. Vlahovska, and M. J. Miksis, Phys. Rev. E **83**, 046309 (2011).
[40] M. I. Angelova and D. S. Dimitrov, Faraday Discuss. Chem. Soc. **81**, 303 (1986).
[41] R. C. Weast, ed., *Handbook of chemistry and physics* (CRC Press, 1988).
[42] M. M. Sadik, J. Li, J. W. Shan, D. I. Shreiber, and H. Lin, Phy. Rev. E. **83**, 066316 (2011).